Catalysis by the Isolated Tryptophan Tryptophylquinone-Containing Subunit of Aromatic Amine Dehydrogenase Is Distinct from Native Enzyme and Synthetic Model Compounds and Allows Fu...

ARTICLE *in* BIOCHEMISTRY · JANUARY 2008

Impact Factor: 3.02 · DOI: 10.1021/bi701690u · Source: PubMed

5 AUTHORS, INCLUDING:

Parvinder Hothi
Swedish Medical Center Seattle
24 PUBLICATIONS **469** CITATIONS
SEE PROFILE

Paul M. Cullis
University of Leicester
175 PUBLICATIONS **3,692** CITATIONS
SEE PROFILE

Nigel S Scrutton
The University of Manchester
346 PUBLICATIONS **7,840** CITATIONS
SEE PROFILE

Catalysis by the Isolated Tryptophan Tryptophylquinone-Containing Subunit of Aromatic Amine Dehydrogenase Is Distinct from Native Enzyme and Synthetic Model Compounds and Allows Further Probing of TTQ Mechanism†

Parvinder Hothi,‡ Michael Lee,§ Paul M. Cullis,§ David Leys,‡ and Nigel S. Scrutton*,‡

Manchester Interdisciplinary Biocentre, Faculty of Life Sciences, University of Manchester, 131 Princess Street, Manchester, M1 7ND, U.K., and Department of Chemistry, University of Leicester, University Road, Leicester, LE1 7RH, U.K.

Received August 21, 2007; Revised Manuscript Received October 5, 2007

ABSTRACT: *Para*-substituted benzylamines are poor reactivity probes for structure−reactivity studies with TTQ-dependent aromatic amine dehydrogenase (AADH). In this study, we combine kinetic isotope effects (KIEs) with structure−reactivity studies to show that *para*-substituted benzylamines are good reactivity probes of TTQ mechanism with the isolated TTQ-containing subunit of AADH. Contrary to the TTQ-containing subunit of methylamine dehydrogenase (MADH), which is catalytically inactive, the small subunit of AADH catalyzes the oxidative deamination of a variety of amine substrates. Observed rate constants are second order with respect to substrate and inhibitor (phenylhydrazine) concentration. Kinetic studies with *para*-substituted benzylamines and their dideuterated counterparts reveal KIEs (>6) larger than those observed with native AADH (KIEs ∼ unity). This is attributed to formation of the benzylamine-derived iminoquinone requiring structural rearrangement of the benzyl side chain in the active site of the native enzyme. This structural reorganization requires motions from the side chains of adjacent residues (which are absent in the isolated small subunit). The position of Pheα97 in particular is responsible for the conformational gating (and hence deflated KIEs) observed with *para*-substituted benzylamines in the native enzyme. Hammett plots for the small subunit exhibit a strong correlation of structure−reactivity data with electronic substituent effects for *para*-substituted benzylamines and phenethylamines, unlike native AADH for which a poor correlation is observed. TTQ reduction in the isolated subunit is enhanced by electron withdrawing substituents, contrary to structure−reactivity studies reported for synthetic TTQ model compounds in which rate constants are enhanced by electron donating substituents. We infer that *para*-substituted benzylamines are good reactivity probes of TTQ mechanism with the isolated small subunit. This is attributed to the absence of structural rearrangement prior to H-transfer that limits the rate of TTQ reduction by *para*-substituted benzylamines in native enzyme.

Tryptophan tryptophylquinone (TTQ[1]) is a novel amino acid-derived cofactor found in the bacterial dehydrogenases aromatic amine dehydrogenase (AADH) and methylamine dehydrogenase (MADH) (*1*−*4*). TTQ is formed by post-translational modification of two gene-encoded tryptophan residues (*5*), and is tightly associated in the enzyme matrix through an amide linkage making it difficult to isolate the intact cofactor from native enzymes (*1*−*6*). Both TTQ-dependent enzymes adopt an $\alpha_2\beta_2$ heterotetrameric structure (α, 40 kDa; TTQ-containing *β*, 14 kDa), and catalyze the oxidative deamination of a wide range of amines to their corresponding aldehydes and ammonia (*2*, *3*). In the reductive half-reaction, two electrons released upon substrate oxidation are transferred to the TTQ cofactor. In the oxidative half-reaction, the TTQ is reoxidized by electron transfer to the type I blue copper proteins azurin (AADH) or amicyanin (MADH), respectively (*2*, *3*).

H-transfer in the reductive half-reaction of both TTQ-dependent dehydrogenases is consistent with full tunneling models of H-transfer and not the Bell tunneling correction model of semiclassical transition state theory (*7*−*10*). The mechanism of the reductive half-reaction of AADH is complex, involving several proton transfers followed by hydrolysis of the Schiff base-reduced TTQ adduct to a *S*-carbinolamine TTQ-adduct (Figure 1). With tryptamine substrate, H-tunneling occurs predominately to the O2 carboxylate of the active site base (Asp128*β*) and is promoted by a short-range motion that modulates the proton-acceptor distance (*9*−*11*). In the oxidative half-reaction, hydrolysis of the product Schiff base produces the aminoquinol intermediate, which is converted back to the oxidized enzyme by two consecutive electron transfers to azurin (*12*). In native AADH, structural reorganization of the substrate-reduced

† The work was funded by the UK Biotechnology and Biological Sciences Research Council. N.S.S. is a BBSRC Professorial Research Fellow.

* Correspondence to this author. Tel: +44 161 306 5152. Fax: +44 161 306 8918. E-mail nigel.scrutton@manchester.ac.uk.

‡ University of Manchester.

§ University of Leicester.

[1] Abbreviations: AADH, aromatic amine dehydrogenase; BisTris, bis(2-hydroxyethyl)iminotris(hydroxymethyl)methane; KIE, kinetic isotope effect; MADH, methylamine dehydrogenase; QSARs, quantitative structure−activity relationships; TTQ, tryptophan tryptophylquinone; σ_p, electronic parameter for substituents in the *para* position; *F*, field/inductive parameter; *R*, resonance parameter.

10.1021/bi701690u CCC: $40.75
Published on Web 12/05/2007

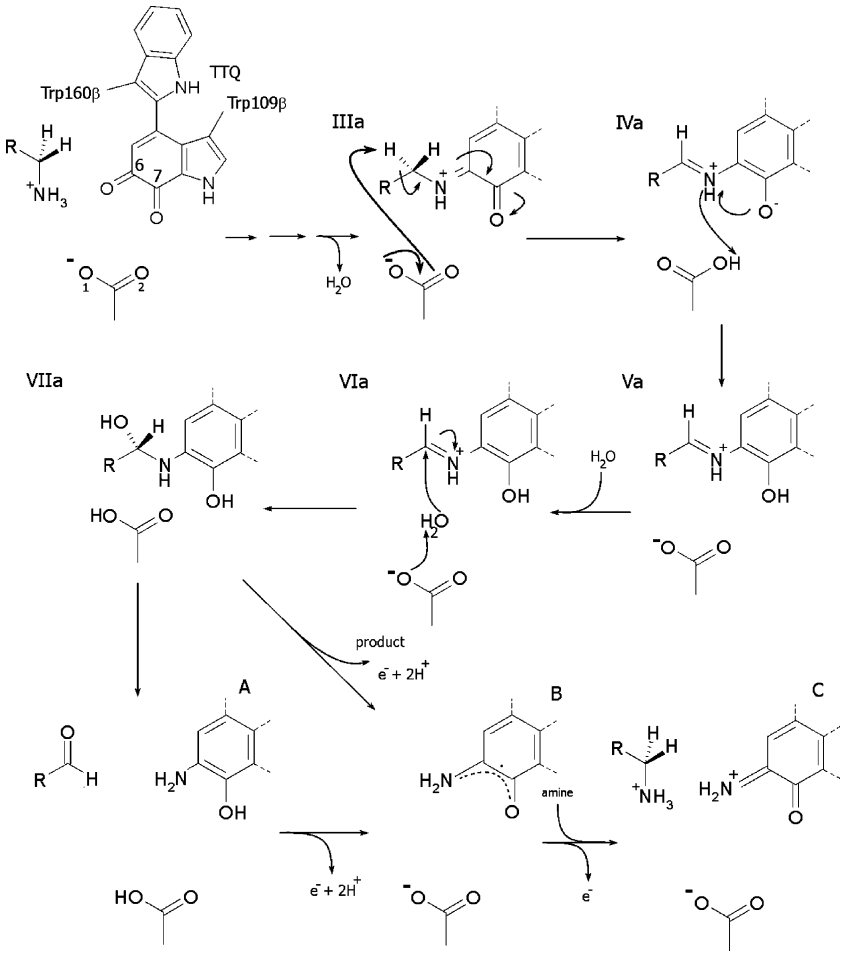

FIGURE 1: Proposed reaction scheme for the reductive half-reaction of AADH with tryptamine as substrate based on crystallographic analysis of reaction intermediates (*9*). Substrate oxidation is dominated by H-tunneling (intermediate **IIIa** to **IV**) and occurs via a multistep mechanism involving several proton transfers (**IVa** to **Va**) followed by hydrolysis of the Schiff base-reduced TTQ adduct (**VIa** to **VIIa**) to a *S*-carbinolamine TTQ adduct (**VIIa**). For clarity only key atoms are represented from intermediate **II** onward, whereas TTQ atoms C6 and C7 and Asp128β O1 and O2 are labeled for intermediate **I**. Broken lines indicate that structures shown are abbreviated for clarity.

small subunit of AADH places a water/ammonia molecule, derived from the initial iminoquinone formation, within hydrogen-bonding distance of the TTQ O7 where it can act as proton acceptor during electron transfer to azurin (*13*, *14*).

Quantitative structure−activity relationships (QSARs) are useful tools for probing enzyme mechanism, and *para*-substituted benzylamines have been employed in the mechanistic interpretation of TTQ-dependent amine dehydrogenases (*15*, *16*). A major limitation, however, is that structure−activity correlations can be compromised in enzyme systems due to complexities in the reaction cycle. We have recently demonstrated this for AADH by combining kinetic isotope effects (KIEs), and crystallographic studies, with structure−reactivity correlations (*17*). Contrary to previous structure−reactivity studies, in which stabilization of a carbanionic intermediate was inferred (*15*, *16*), we showed that *para*-substituted benzylamines are poor probes of quinoprotein mechanism for AADH (*17*). We have identified major structural reorganization in the active site, prior to C−H bond breakage, that compromises the rate of TTQ reduction and accounts for the deflated KIEs observed with benzylamine substrates (Figure 2) (*17*).

In addition to structure−activity correlations as probes of TTQ mechanism, several indolequinone derivatives have been synthesized to represent non-protein bound models of TTQ (*18*−*23*). The model compounds have molecular geometries, redox potentials, and spectroscopic properties similar to those of the native enzymes (*18*−*21*). The model chemistry, however, relies on excess substrate to act as proton acceptor (*20*) whereas the enzyme chemistry utilizes an active site aspartate residue (*9*). Amine oxidation by the model compounds is considerably slower than the enzyme-catalyzed reactions (*19*−*22*), but the reaction mechanism is consistent with the proposed mechanism for TTQ-dependent amine dehydrogenases (*15*, *16*, *24*). Synthetic TTQ is readily transformed into an iminoquinone-type adduct through reaction with ammonia (*19*) or cyclopropylamine (*20*). With benzylamine substrates, formation of the iminoquinone adduct is followed by rearrangement to the product imine, which is then converted into the aminophenol (*20*). Although the isotope effect for C−H bond breakage in the TTQ model chemistry is substantial (∼9), studies of the temperature dependence of the KIE have not been reported (*20*).

We report the first kinetic study of a TTQ-containing subunit isolated from an amine dehydrogenase. By investigating the KIE, and temperature (in)dependence of the KIE, we are able to compare kinetic and thermodynamic data with our existing data for the enzyme-catalyzed reaction (which is dominated by H-tunneling). Given that *para*-substituted benzylamines are poor probes of quinoprotein mechanism

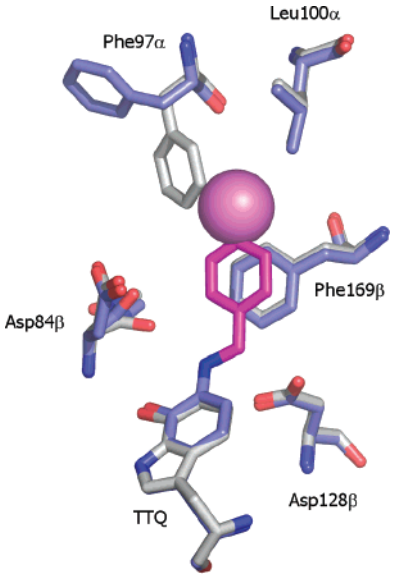

FIGURE 2: The proposed *para*-substituted benzylamine intermediate III structure for native AADH (*17*). The benzylamine-derived iminoquinone requires structural rearrangement of the benzyl side chain, which can only occur if corresponding motions occur for the side chain of Pheα97 in addition to the Aspα84 backbone. The required reorganization is larger with *para*-substituted benzylamines, and additional motions (i.e., of Leuα100) are required to accommodate larger substituents. Active site residues are depicted in atom colored sticks with the *para*-substituted benzylamine substrate in magenta carbons (protein carbons are in light blue). For comparison, corresponding positions of key active site amino acids in the benzylamine−AADH complex are superimposed depicted with gray carbons. The position of the *para* substituent is depicted by a large magenta sphere (*17*).

for AADH (*17*), and that structure−reactivity correlations for TTQ model compounds exhibit a negative correlation (*20*), we investigate structure−activity relationships with the isolated small subunit. From our kinetic and crystallographic studies with native enzyme, which have identified major structural reorganization in the active site prior to C−H bond breakage (*17*), we are able to attribute the larger KIEs (>6) observed with the small subunit to the absence of structural rearrangement prior to H-transfer. We thus infer that *para*-substituted benzylamines are good reactivity probes of TTQ mechanism with the isolated small subunit.

EXPERIMENTAL PROCEDURES

Materials. BisTris propane, tryptamine, phenethylamine, hydroxyphenethylamine, nitrophenethylamine, benzylamine and *para*-substituted benzylamines were obtained from Sigma. Amino, methyl, fluoro and chlorophenethylamines were from Acros Organics. Bromophenethylamine was obtained from Fluorochem and methoxyphenethylamine from Apollo Scientific Ltd. Guanidine hydrochloride was from Invitrogen. Deuterated tryptamine HCl (tryptamine-β,β-d_2 HCl, 98%), deuterated phenethylamine ($C_6D_5CD_2CD_2NH_2$, 98%) and deuterated benzylamine HCl ($C_6D_5CD_2NH_2$ HCl, 99.6%) were obtained from CDN Isotopes. The chemical purity of the deuterated reagents was determined to be >98% by high performance liquid chromatography, NMR, and gas chromatography, by the suppliers. Dideuterated *para*-substituted benzylamines (90−99% isotopically enriched) were synthesized as described (*17*).

Purification of AADH and Isolation of the Small Subunit. Alcaligenes faecalis IFO 14479 was grown aerobically at 30 °C on 0.15% (w/v) phenethylamine (*25*), and AADH was purified as described previously (*26*). For isolation of the small subunit, AADH was incubated in 5 M guanidine hydrochloride for ~30 h at room temperature. The enzyme was applied to a Sephacryl S-200 gel filtration column equilibrated with 10 mM potassium phosphate buffer, pH 7.5, containing 100 mM KCl and 1 M guanidine hydrochloride. Fractions containing the small subunit were concentrated by ultrafiltration (10 kDa cutoff) and dialyzed against 10 mM potassium phosphate, pH 7.5. The small subunit was stored at −80 °C in 10 mM potassium phosphate buffer, pH 7.5, with 10% ethylene glycol.

Prior to use in kinetic studies, AADH and the small subunit were reoxidized with potassium ferricyanide and exchanged into 10 mM BisTris propane buffer, pH 7.5, by gel exclusion chromatography. AADH concentration was determined using an extinction coefficient of 27,600 M^{-1} cm^{-1} at 433 nm (*1*). The concentration of the small subunit was determined using an extinction coefficient of 10,700 M^{-1} cm^{-1} at 420 nm. This is similar to the extinction coefficient (ϵ_{410} = 11,000 M^{-1} cm^{-1}) reported for the small subunit of MADH (*27*).

Anaerobic Titrations of the Small Subunit of AADH. Anaerobic experiments were performed in a Belle Technology glove box (<5 ppm of oxygen). Buffer was made anaerobic by bubbling with argon for 2 h and left to equilibrate overnight in the glove box. Anaerobic solutions of substrate were prepared by dissolving preweighed solid in anaerobic buffer. The small subunit of AADH was reoxidized with potassium ferricyanide and exchanged into anaerobic 10 mM BisTris propane buffer, pH 7.5, by gel exclusion chromatography. Following addition of substrates (see Results), spectra were recorded using a Jasco V-550 UV/vis spectrophotometer housed in the glove box.

Kinetic Studies of the Reductive Half-Reaction. Rapid kinetic experiments were performed using an Applied Photophysics SX.18MV stopped-flow spectrophotometer. Studies of TTQ reduction were performed by rapid mixing of oxidized small subunit (reaction cell concentration 2 μM) in 10 mM BisTris propane buffer, pH 7.5, with various concentrations of substrate (see Results), at 25 °C. Reduction of the TTQ cofactor was followed at 420 nm. Data were analyzed by nonlinear least-squares regression analysis on an Acorn RISC PC using Spectrakinetics software (Applied Photophysics). For each reaction, at least three replicate measurements were collected and averaged, each containing 1000 data points. Slow reactions requiring longer than 1000 s (see Results) were followed spectroscopically using a Jasco V-550 UV/vis spectrophotometer. Absorbance changes accompanying reduction were monophasic or biphasic, and observed rates were obtained by fitting to the standard single or double exponential expression. For AADH, kinetic studies were performed by rapid mixing of oxidized AADH (reaction cell concentration 1 μM) in 10 mM BisTris propane buffer, pH 7.5, with various concentrations of substrate (see Results), at 25 °C. Reduction of the TTQ cofactor in AADH was followed at 456 nm as described previously (*26*). Where appropriate, the concentration dependence of k_{obs} was analyzed by fitting to the standard hyperbolic expression (*28*) to obtain values for the apparent dissociation constant for

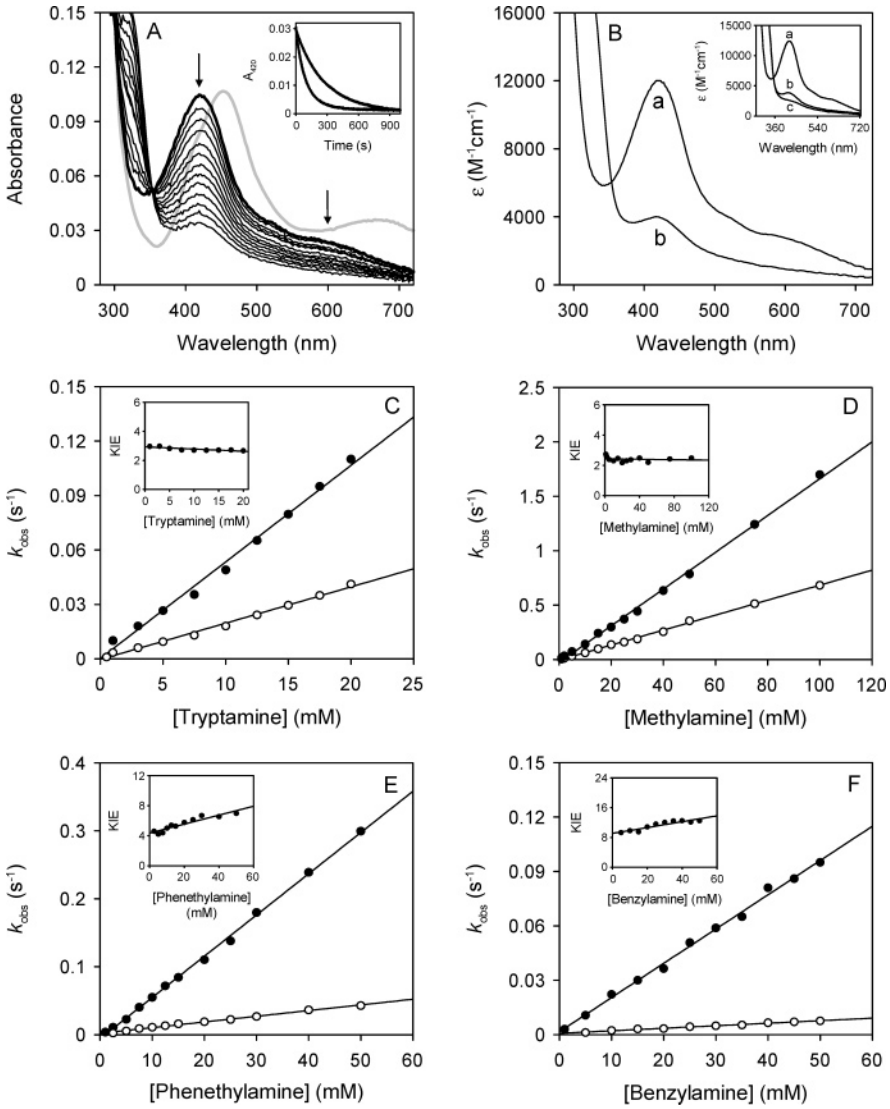

FIGURE 3: Spectral and kinetic properties of the small subunit of AADH. Panel A: Spectral changes accompanying reduction of the isolated subunit. The subunit (10 μM), in 10 mM BisTris propane buffer (pH 7.5), was reduced by addition of methylamine (5 mM) at 25 °C. For comparison, the absorption spectrum of oxidized AADH (3.5 μM) is shown in gray. Inset: Example of the absorbance change monitored at 420 nm during single wavelength studies of the reductive half-reaction (kinetic data presented in panels C−F). Conditions: 2.5 μM small subunit, 1 mM protiated or deuterated tryptamine, 10 mM BisTris propane buffer, pH 7.5, at 25 °C. Panel B: photodiode array studies of subunit reduction. The small subunit (10 μM) was rapidly mixed with 5 or 50 mM methylamine at 25 °C. Spectral changes accompanying small subunit reduction are as in panel A. Spectral intermediates were identified by global analysis by fitting to a one step kinetic model. Spectrum a is the oxidized species, and spectrum b is the reduced species. Inset: Spectral intermediates identified by fitting to a two step kinetic model for halogen-substituted amines that displayed double exponentials on reduction. Panel C: Kinetic data for reduction of the small subunit by tryptamine. Filled circles, k_{obs} for protiated tryptamine; open circles, k_{obs} for deuterated tryptamine. Inset: plot of ln KIE versus substrate concentration for the kinetic data presented in the main panel. Conditions: 2 μM of small subunit (reaction cell concentration) in 10 mM BisTris propane buffer, pH 7.5, at 25 °C. Panels D, E and F: As for panel C but for methylamine, phenethylamine and benzylamine, respectively. Observed rates were obtained by fitting to the standard single-exponential expression.

the enzyme−substrate complex, K_d, and the limiting rate, k_{lim}, of TTQ reduction.

In studies of the temperature dependence of bond breakage, the small subunit was equilibrated in the stopped-flow apparatus (or in the UV−visible spectrophotometer for slower reactions) at the appropriate temperature prior to the acquisition of kinetic data. Temperature control was achieved using a thermostatic circulating water bath, and the temperature was monitored directly in the stopped-flow apparatus using a semiconductor sensor (or a thermometer in the UV/visible spectrophotometer). Kinetic and thermodynamic parameters were obtained by fitting data to the unimolecular Eyring equation as described and rationalized previously for TTQ-dependent methylamine dehydrogenase (*7*).

For multiple wavelength studies, the small subunit (reaction cell concentration ~10 μM) contained in 10 mM BisTris propane buffer, pH 7.5, was rapidly mixed with substrate (see Results) at 25 °C. Multiple-wavelength absorption studies were performed using a photodiode array detector and X-SCAN software (Applied Photophysics). Spectra were analyzed and intermediates of the reaction identified by global analysis and numerical integration methods using PROKIN software (Applied Photophysics).

Inactivation of AADH and the Small Subunit by Phenylhydrazine. Stoichiometric concentrations of phenylhydrazine (16 μM and 20 μM) were added to AADH (8 μM) and the small subunit (10 μM), respectively, in 10 mM BisTris propane buffer, pH 7.5. Spectral changes observed on

Table 1: KIEs and Second-Order Rate Constants (k_1) Determined for Reactions of the Small Subunit of AADH with Amine Substrates at 25 °C[a]

substrate	k_1^H (M^{-1} s^{-1})	k_1^D (M^{-1} s^{-1})	k_{obs}^H (s^{-1})	k_{obs}^D (s^{-1})	KIE
benzylamine	1.9 ± 0.1	0.14 ± 0.01	0.042 ± 0.01	0.004 ± 0.01	10.5 ± 1.0
phenethylamine	6.1 ± 0.1	0.8 ± 0.01	0.11 ± 0.01	0.019 ± 0.01	5.8 ± 0.3
tryptamine	5.3 ± 0.2	2.0 ± 0.1	0.11 ± 0.01	0.041 ± 0.01	2.7 ± 0.2
methylamine	16.9 ± 0.3	6.9 ± 0.1	0.3 ± 0.02	0.13 ± 0.01	2.3 ± 0.2
ethanolamine	6.3 ± 0.1	-	0.063 ± 0.01	-	-
dopamine	4.1 ± 0.1	-	0.11 ± 0.01	-	-

[a] Rate constants (k_{obs}) are values determined at a substrate concentration of 20 mM from which the KIE is determined.

addition of phenylhydrazine were recorded using a Jasco V-550 UV/vis spectrophotometer. Single wavelength kinetic studies were performed using an Applied Photophysics SX.18MV stopped-flow spectrophotometer. AADH (reaction cell concentration 2 μM) or the small subunit (4 μM) was rapidly mixed with various concentrations of phenylhydrazine at 25 °C. Formation of the TTQ−phenylhydrazine complex was followed as an increase in absorbance at 528 nm. Absorbance changes were biphasic, and observed rate constants were thus obtained by fitting to the standard double exponential expression.

RESULTS

Kinetic Studies of TTQ Reduction in the Catalytic Subunit of AADH. We have recently reported a comprehensive description of the overall reaction pathway, in particular the H-tunneling step, of AADH using X-ray crystallography, kinetic and computational methods (*9*). Our kinetic studies with AADH have identified large variation in the limiting rate of TTQ reduction with different amine substrates, and a wide range of KIEs associated with breakage of the substrate C−H/C−D bond (*8*, *9*, *17*). Herein, we have extended kinetic studies of amine dehydrogenase-type reactions by characterization of the TTQ-containing small subunit of AADH.

The small subunit of AADH was isolated as described in Experimental Procedures. NMR analysis revealed that the small subunit adopts a compact globular fold, with no evidence for any highly mobile or unfolded regions (Figure S1 in Supporting Information). The UV−visible absorption spectrum of the small subunit is different from that of the native enzyme (Figure 3A) but highly similar to the small subunit of MADH (*4*). Absorption maximum at 420 nm (compared to 456 nm for native AADH) is lost on reduction of the TTQ cofactor. Kinetic studies were therefore performed by following absorbance changes at 420 nm on mixing of oxidized small subunit with various amine substrates at 25 °C. Where appropriate, reactions were monitored using the stopped-flow apparatus. Reactions requiring longer than 1000 s (low substrate concentrations, slow, or deuterated substrates) were monitored in a spectrophotometer. Absorbance changes accompanying reduction (Figure 3A inset) were either monophasic or biphasic, and observed rates were obtained by fitting to the expression describing a single or double exponential as appropriate. The fast phase of biphasic transients (~85% of the total amplitude change) exhibits the KIE.

Observed rate constants (k_{obs}) for TTQ reduction in the small subunit showed a linear dependence on substrate concentration (Figure 3C−F). Rate constants and KIEs

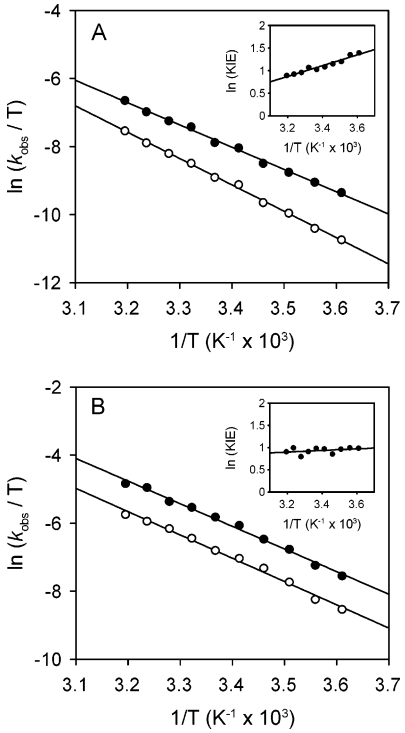

FIGURE 4: Eyring plots for reactions of the small subunit of AADH with various amine substrates. Panel A: Plot of ln k_{obs}/T versus $1/T$ for reduction of the small subunit by tryptamine and deuterated tryptamine. Filled circles, protiated tryptamine; open circles, deuterated tryptamine. Inset: Plot of ln KIE versus $1/T$ for the kinetic data presented in the main panel. Conditions: 2 μM small subunit, 10 mM BisTris propane buffer, pH 7.5, 4−40 °C. Rate constants are observed rate constants measured using 20 mM tryptamine. Observed rates were obtained by fitting to the standard single (<28 °C) or double exponential expression. For each reaction at least four replicate measurements were collected and averaged. Similar data were obtained with 5 mM tryptamine (Table 2; Figure S3 in the Supporting Information). Panel B: As for panel A but with 50 mM methylamine as substrate. One standard deviation in each activity measurement ($n = 4$) at a defined temperature is <10% of the determined value. Kinetic and thermodynamic parameters (Table 2) were obtained from fitting data to the Eyring equation.

determined for several amines are summarized in Table 1. For AADH, tryptamine is the "fastest" substrate in the reductive half-reaction [second-order rate constant: 3.13 ± 0.12 × 10^7 M^{-1} s^{-1} at 4 °C] and methylamine is significantly slower [1.9 ± 0.03 × 10^2 M^{-1} s^{-1} at 25 °C (data not shown)]. In the small subunit, however, methylamine is the "fastest" substrate with a second-order rate constant of 16.9 ± 0.3 M^{-1} s^{-1} (compared to 5.3 ± 0.2 M^{-1} s^{-1} for tryptamine). For tryptamine and methylamine dependent reactions with the subunit, KIEs (2.7 ± 0.2 and 2.3 ± 0.2, respectively)

Table 2: Kinetic and Thermodynamic Parameters Determined for Reactions of the Small Subunit of AADH with Amine Substrates[a]

substrate	[substrate] (mM)	$\Delta H^{\ddagger H}$ (kJ mol^{-1})	$\Delta H^{\ddagger D}$ (kJ mol^{-1})	$\Delta\Delta H^{\ddagger}$ (kJ mol^{-1})	A'^{H}:A'^{D}	KIE at 24 °C
tryptamine	5	51.8 ± 1.8	58.0 ± 1.4	6.2 ± 3.2	0.19 ± 0.02	2.4 ± 0.2
tryptamine	20	54.4 ± 1.2	64.3 ± 1.0	9.9 ± 2.2	0.05 ± 0.003	2.79 ± 0.3
methylamine	5	52.5 ± 0.8	57.9 ± 1.8	5.4 ± 2.6	0.26 ± 0.02	2.59 ± 0.2
methylamine	50	55.3 ± 1.6	56.9 ± 1.8	1.6 ± 3.4	1.32 ± 0.13	2.67 ± 0.2
phenethylamine	50	61.2 ± 1.6	74.8 ± 1.4	13.6 ± 3.0	0.02 ± 0.002	6.79 ± 0.7
benzylamine	50	61.6 ± 1.0	69.1 ± 1.0	7.5 ± 2.0	0.47 ± 0.05	9.5 ± 1.0

[a] Reactions were monitored in the temperature range of 4 to 40 °C. Parameters were obtained from fitting data to the Eyring equation.

are independent of substrate concentration.[2,3] KIEs for phenethylamine and benzylamine are significantly larger (at 20 mM, 5.8 ± 0.3 and 10.5 ± 1.0, respectively) but the magnitude of the KIE is dependent on substrate concentration with these amines (Figure 3E, F). The origin of this phenomenon remains unclear. We have observed inflated KIEs for the reductive half-reaction of native enzyme with tryptamine (55 ± 6) (*8*, *9*) and dopamine (12.9 ± 0.2) (*8*), and a considerably deflated KIE with benzylamine (4.6 ± 0.2) (*8*, *26*). The opposite scenario is observed with the small subunit of AADH (KIEs of 2.7 and 10.5 for tryptamine and benzylamine, respectively; Table 1).

Photodiode array detection revealed that spectral changes accompanying reduction of the small subunit by tryptamine and methylamine were best described by a one step kinetic model A → B (Figure 3B) by global analysis (species a is the oxidized small subunit, and species b is the reduced species). Parameters determined from photodiode array studies were similar to those obtained during single wavelength studies (e.g., 20 mM protiated and deuterated tryptamine had observed rate constants of 0.12 ± 0.001 s^{-1} and 0.05 ± 0.001 s^{-1}, respectively [KIE = 2.7]). For substrates that displayed biphasic absorbance changes during single wavelength studies (i.e., some *para*-substituted amines; see Structure−Reactivity Correlations), intermediates determined from fitting to a two step kinetic model A → B → C (Figure 3B inset) are shown. It should be noted that, given the small absorbance change associated with B → C (~15% of the total amplitude change), and very slow rate constant (0.02 s^{-1}), it is difficult to clearly distinguish between monophasic and biphasic kinetics for some amine substrates. Control studies of the small subunit versus buffer revealed no spectral changes in the absence of substrate.

Temperature Dependence Studies and Kinetic Isotope Effects. Temperature dependence studies were performed with the small subunit to allow comparison of kinetic and thermodynamic parameters determined previously for the native enzyme. Eyring plots for the small subunit indicate that the KIE is dependent on temperature for reactions with tryptamine (5 and 20 mM), methylamine (5 mM), phenethylamine (50 mM) and benzylamine (50 mM) [Figure 4A and Figure S3 in Supporting Information]. Eyring plots obtained with a higher concentration of methylamine (50 mM) indicate a measurably temperature-independent KIE (Figure 4B). Kinetic and thermodynamic parameters were obtained by fitting data to the Eyring equation and are summarized in Table 2. Values of $\Delta H^{\ddagger H}$ (but not $\Delta H^{\ddagger D}$) are similar to those obtained for reactions of native enzyme with tryptamine ($\Delta H^{\ddagger H}$ = 57.3 ± 3.4 kJ mol^{-1}, $\Delta H^{\ddagger D}$ = 53.5 ± 1.2 kJ mol^{-1}), phenethylamine ($\Delta H^{\ddagger H}$ = 54.7 ± 0.6 kJ mol^{-1}, $\Delta H^{\ddagger D}$ = 54.3 ± 0.7 kJ mol^{-1}), and benzylamine ($\Delta H^{\ddagger H}$ = 68.1 ± 1.4 kJ mol^{-1}, $\Delta H^{\ddagger D}$ = 64.3 ± 1.0 kJ mol^{-1}).[4] The larger $\Delta H^{\ddagger D}$ values for reactions of the small subunit lead to $\Delta\Delta H^{\ddagger}$ of ~10 ± 3 kJ mol^{-1} (Table 2), unlike thermodynamic parameters obtained with native enzyme ($\Delta\Delta H^{\ddagger}$ ~0 ± 5 kJ mol^{-1}) (*8*, *9*) [see Discussion].

Structure−Reactivity Correlations. Para-substituted benzylamines are poor reactivity probes for structure−reactivity studies with AADH owing to major structural reorganization in the active site, which compromises the rate of TTQ reduction by benzylamine substrates (*17*). A poor correlation of TTQ reduction with electronic substituent effects and KIEs of unity are therefore observed with the native enzyme (*17*). However, kinetic studies of the isolated small subunit with *para*-substituted benzylamines and their dideuterated counterparts reveal larger KIEs (Figure 5A and Table 3). Given that KIEs greater than unity are observed for reactions catalyzed by the small subunit (suggesting the absence of structural reorganization as with native enzyme; see Discussion), we have performed structure−reactivity studies of the small subunit with *para*-substituted benzylamines and phenethylamines. To probe the influence of electronic properties on TTQ reduction, observed rate constants were correlated with electronic (σ_p), field/inductive (*F*) and resonance (*R*) effects. Substituent constants were obtained from (*29*) and (*30*). The *R* and *F* constants are modified Swain−Lupton constants that have been adjusted to the same scale as the Hammett constants (*30*). Reactions were performed as described in Kinetic Studies of TTQ Reduction in the Catalytic Subunit of AADH (Figure 5B, C), and Hammett plots were constructed by plotting the logarithm of the observed rate constant (Table 4) versus σ_p, *F* and *R* parameters. An increase in electronegativity is represented by negative to positive sigma (σ_p) values in Hammett plots.

For AADH, the breakdown in structure−reactivity correlations is more obvious with *para*-substituted phenethylamines than with benzylamine substrates, possibly due to field/inductive effects being attenuated with distance (*17*). For the small subunit, we observe a stronger correlation for log k_{obs} versus electronic effects (Figure 6A, B), and field/

[2] It was not possible to accurately measure rates with more than 20 mM tryptamine due to solubility problems with this substrate. Reactions with methylamine, however, were performed with 1−100 mM, and the KIE remained independent of substrate concentration within this range.

[3] Steady-state reactions of the small subunit with methylamine show a similar linear dependence on substrate concentration and a substrate independent KIE of 2.2 ± 0.2 (Figure S2 in Supporting Information).

[4] $\Delta H^{\ddagger}$ values for reactions of AADH with tryptamine, phenethylamine and benzylamine are taken from (*9*), Hothi, P. & Scrutton, N. S., unpublished data, and (*26*), respectively.

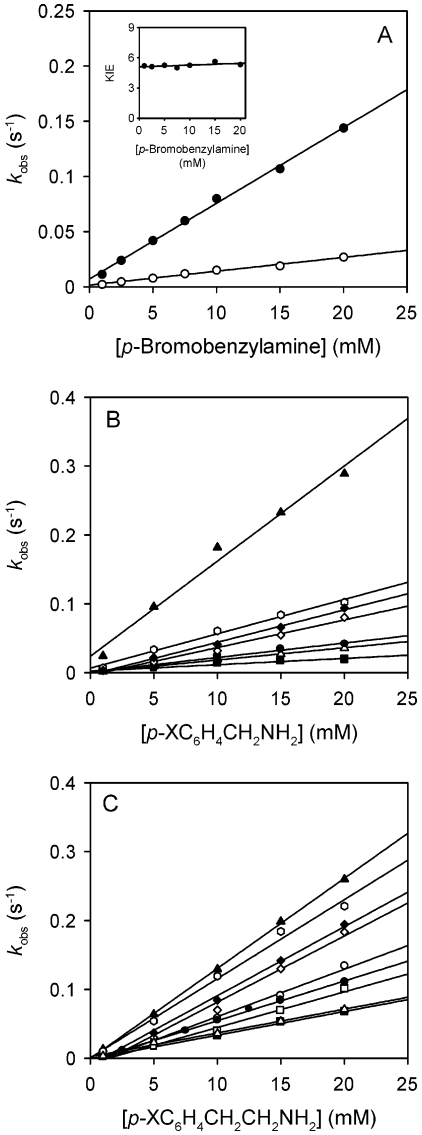

FIGURE 5: Kinetic data for reactions of the small subunit with *para*-substituted amines. Panel A: Reactions of the small subunit with bromobenzylamine. Filled circles, protiated bromobenzylamine; open circles, deuterated bromobenzylamine. Inset: Plot of ln KIE versus substrate concentration for the kinetic data presented in the main panel. Conditions: 2 μM of small subunit in 10 mM BisTris propane buffer, pH 7.5, at 25 °C. Observed rates were obtained by fitting to the double exponential expression. Panel B: Kinetic data for reactions of the small subunit with *para*-substituted benzylamines. Filled circles, benzylamine; open triangles, methoxy; filled triangles, nitro; filled diamonds, chloro; filled squares, methyl; open diamonds, fluoro; open hexagons, bromobenzylamine. Panel C: As for panel B but for *para*-substituted phenethylamines. Filled circles, phenethylamine; open triangles, methoxy; filled triangles, nitro; filled diamonds, chloro; open circles, hydroxy; open squares, amino; filled squares, methyl; open diamonds, fluoro; open hexagons, bromophenethylamines. Reactions were performed as described for panel A, and observed rates were obtained by fitting to the standard single or double exponential expression (for methoxy and halogen substituted amines).

inductive effects (Figure 6C, D). Moreover, we demonstrate that structure−reactivity correlations are similar with *para*-substituted benzylamines and phenethylamines (i.e., no difference from field/inductive effects being attenuated with distance for reactions with the small subunit). The nitro substituent (most electron withdrawing group) activates bond cleavage, and the methyl substituent (that donates electrons toward the cleavable bond) has the slowest rate for TTQ reduction (Table 4). For reactions of AADH with nitrobenzylamine, bond cleavage is activated ~30-fold but not with nitrophenethylamine (Table 4). For reactions with the small subunit, bond cleavage is activated to the same degree (Table 4) with nitrobenzylamine (13.8 ± 0.9 M^{-1} s^{-1}) and nitrophenethylamine (13.1 ± 0.1 M^{-1} s^{-1}). The breakdown in structure−reactivity correlations with AADH is owing to the rates of TTQ reduction observed with the *para*-substituted halogen benzylamines. The halogen substituents have similar *F* constants thus, for strong correlations between field/inductive effects and TTQ reduction, similar k_{lim} values are expected with these substrates. However, observed rate constants vary (~1.4 s^{-1} for chloro- and bromobenzylamines compared to 5.5 s^{-1} for fluorobenzylamine; Table 4), causing deviation from linear behavior in Hammett plots (*17*). For the small subunit, rate constants are similar with the halogen-substituted amines (Table 4), resulting in a more linear dependence in Hammett plots. A weak correlation was observed for log k_{obs} versus resonance effects (*R*) for *para*-substituted benzylamines and phenethylamines (Figure 6E, F).

Kinetic Studies of TTQ Reduction in AADH and the Small Subunit with Difluoro- and Dimethoxybenzylamines. Studies of the reductive half-reaction of AADH and the small subunit were also performed with 2,4-difluorobenzylamine and 2,4-dimethoxybenzylamine. Addition of dimethoxybenzylamine

Table 3: KIEs Determined for Reactions of the Small Subunit of AADH with *Para*-Substituted Benzylamines at 25 °C[a]

para-substituent	AADH	small subunit
H	4.59 ± 0.2	9.8 ± 1.0
CH_3	1.16 ± 0.1	7.7 ± 0.8
OCH_3	5.41 ± 0.1	9.2 ± 1.1
NO_2	1.63 ± 0.1	6.2 ± 0.8
F	6.05 ± 0.1	10.7 ± 1.2
Cl	1.41 ± 0.1	9.6 ± 1.0
Br	1.49 ± 0.1	5.8 ± 0.6

[a] KIEs for reactions of native AADH with benzylamine substrates are taken from Hothi et al. (*17*). For reactions catalyzed by the small subunit, KIEs are determined from observed rate constants measured at a substrate concentration of 10 mM. For each reaction, at least three replicate measurements were collected and averaged. Higher concentrations were not used due to limited availability of the dideuterated benzylamines.

Table 4: Kinetic Parameters Determined for Reactions of AADH and the Small Subunit of AADH with *Para*-Substituted Amines at 25 °C[a]

	phenethylamine		benzylamine	
para-substituent	AADH k_{lim} (s^{-1})	small subunit k_1 (M^{-1} s^{-1})	AADH k_{lim} (s^{-1})	small subunit k_1 (M^{-1} s^{-1})
H	45.56 ± 0.3	6.1 (0.11)	1.47 ± 0.01	2.0 (0.04)
CH_3	44.7 ± 0.3	3.4 (0.07)	0.29 ± 0.01	0.9 (0.02)
OCH_3	417.6 ± 10.7	3.5 (0.07)	5.09 ± 0.04	1.8 (0.04)
NO_2	29.35 ± 0.2	13.1 (0.26)	48.7 ± 0.41	13.8 (0.29)
F	93.13 ± 0.7	9.6 (0.18)	5.51 ± 0.04	4.0 (0.08)
Cl	65.5 ± 0.3	10.0 (0.19)	1.37 ± 0.01	4.7 (0.09)
Br	73.8 ± 0.3	11.5 (0.22)	1.40 ± 0.02	4.9 (0.1)
OH	412.7 ± 7.0	6.9 (0.14)		
NH_2	31.6 ± 0.3	5.2 (0.10)		

[a] The limiting rates of TTQ reduction for AADH are taken from Hothi et al. (*17*). For reactions catalyzed by the small subunit, numbers in parentheses are observed rate constants (k_{obs}) determined at a substrate concentration of 20 mM. Errors associated with second-order rate constants (k_1) and k_{obs} (s^{-1}) are <10% of the determined value.

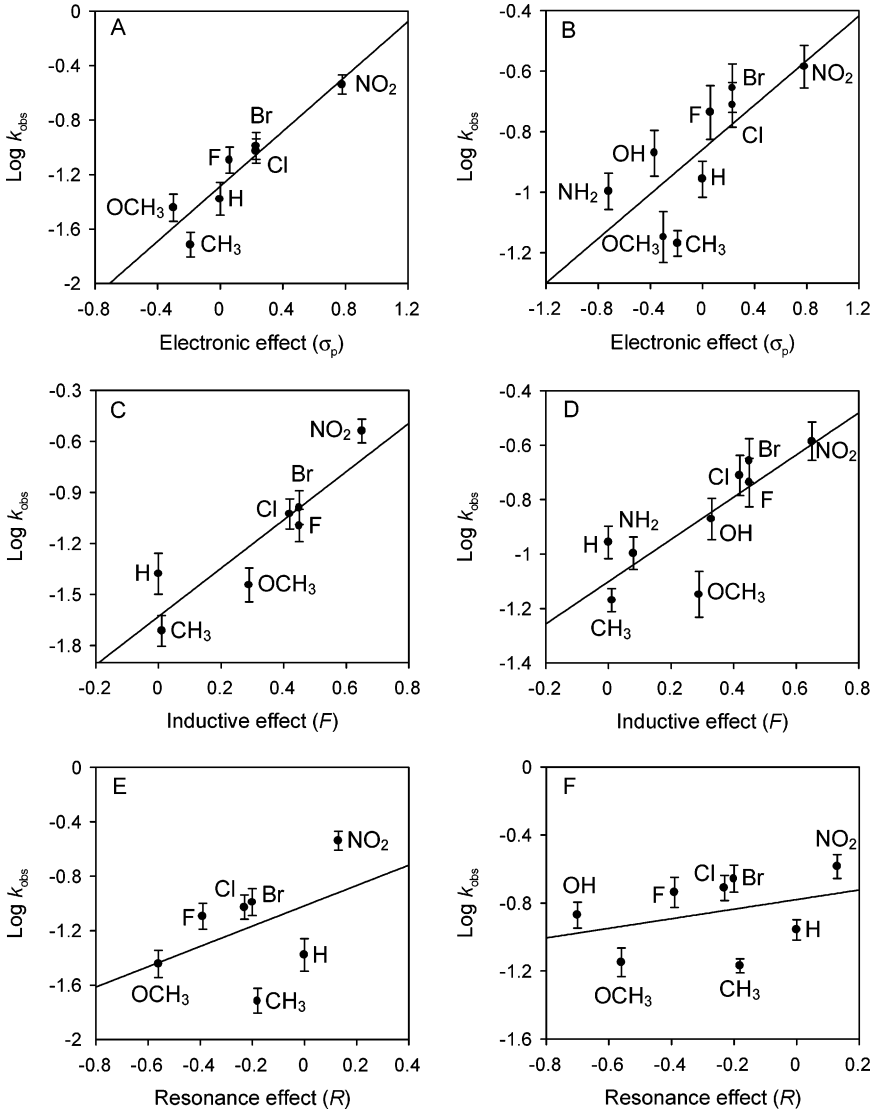

FIGURE 6: Hammett plots for structure−reactivity correlations in the small subunit of AADH. Panels A, B: Plots of log k_{obs} versus electronic effects (σ_p) for reactions of the small subunit with *para*-substituted benzylamines and phenethylamines, respectively. Reactions were performed as described in the legend of Figure 4. Panels C, D: Hammett plots of log k_{obs} versus field/inductive effects (F) for reactions of the small subunit with *para*-substituted benzylamines and phenethylamines, respectively. Panels E, F: Hammett plots of log k_{obs} versus resonance effects (R) for reactions of the small subunit with *para*-substituted benzylamines and phenethylamines, respectively. Observed rate constants (k_{obs}) used for Hammett plots are values determined at a substrate concentration of 20 mM (Table 3).

to AADH revealed a shift in maximum absorbance from 456 to 464 nm but no reduction of the TTQ cofactor (Figure 7A). The small subunit revealed a similar spectral shift (420 to 423 nm or 429 nm with 10 and 50 mM dimethoxybenzylamine, respectively), but complete TTQ reduction was observed (Figure 7B). Absorbance changes accompanying AADH reduction with difluorobenzylamine were monophasic. The plot of observed rate constant against difluorobenzylamine concentration is shown in Figure 7C (k_{lim}, 2.03 ± 0.01 s^{-1}; K_d, 43.8 ± 1.6 μM). Kinetic data for reactions of the subunit with difluorobenzylamine (second-order rate constant: 0.9 ± 0.01 M^{-1} s^{-1}) and dimethoxybenzylamine (0.12 ± 0.01 M^{-1} s^{-1}) are shown in Figure 7D.

Inactivation of AADH and the Small Subunit by Phenylhydrazine. Hydrazines are known to inhibit a wide range of redox enzymes (*31*). In AADH and MADH, inactivation by phenylhydrazine involves nucleophilic attack by the hydrazine nitrogen on the C6 carbonyl carbon of the TTQ cofactor, forming a covalent hydrazone adduct (*1*, *32*). Spectral changes observed on addition of phenylhydrazine to AADH (Figure 8A inset) are similar to those observed for the small subunit (Figure 8A), suggesting similar adduct formation. AADH (reaction cell concentration 2 μM) or the small subunit (4 μM) was rapidly mixed with various concentrations of phenylhydrazine at 25 °C. Formation of the TTQ−phenylhydrazine complex was followed at 528 nm. In both cases, an increase in absorbance was observed at 528 nm. Absorbance changes were biphasic, and observed rate constants were obtained by fitting to the standard double exponential expression. At 500 μM phenylhydrazine, rate constants of k_{obs1} (s^{-1}) = 436 ± 28.6, k_{obs2} (s^{-1}) = 47.7 ± 3.6 and k_{obs1} (s^{-1}) = 0.11 ± 0.01, k_{obs2} (s^{-1}) = 0.005 ± 0.001 were obtained for AADH and the small subunit, respectively. A hyperbolic dependence is observed for AADH (k_{lim}, 644.2 ± 28.6 s^{-1}; K_d, 247.2 ± 24.8 μM; Figure 8B inset) and a linear dependence (2.49 ± 0.1 × 10^2 M^{-1} s^{-1}) for the small subunit (Figure 8B). As observed for kinetic studies with amine substrates, no K_d value can be obtained for the small subunit−phenylhydrazine complex.

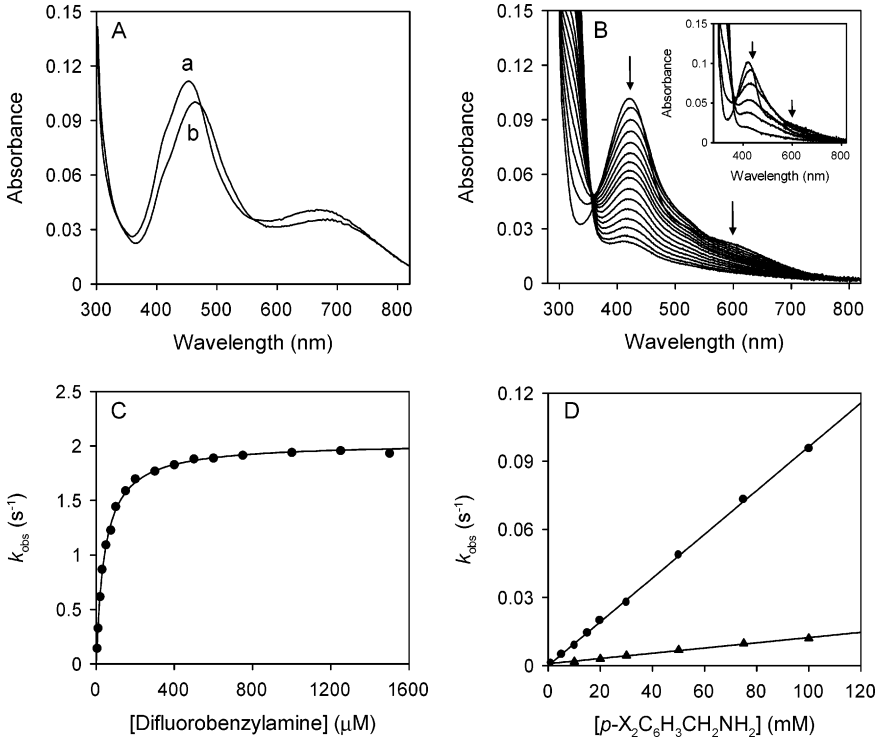

FIGURE 7: Kinetic properties of AADH and the small subunit with disubstituted benzylamines. Panel A: Spectral change accompanying the addition of dimethoxybenzylamine (500 μM) to AADH (4 μM). Spectrum a is the oxidized enzyme (maximum absorbance at 456 nm), and spectrum b is the species observed on addition of dimethoxybenzylamine (maximum absorbance shifts to 464 nm). Panel B: Spectral changes accompanying the addition of dimethoxybenzylamine (10 mM) to the small subunit of AADH (8 μM). Maximum absorbance shifts from 420 to 423 nm. Inset: As main panel but with 50 mM dimethoxybenzylamine. Maximum absorbance shifts from 420 to 429 nm. Panel C: Stopped-flow kinetic data for the reductive half-reaction of AADH with difluorobenzylamine. Conditions: 1 μM AADH in 10 mM BisTris propane buffer, pH 7.5, 25 °C. Observed rates were obtained by fitting to the standard single-exponential expression. The fit shown is to the standard hyperbolic expression. Panel D: Kinetic data for the reaction of the small subunit with disubstituted benzylamines. Filled circles, difluorobenzylamine; filled triangles, dimethoxybenzylamine. Conditions: 2 μM small subunit in 10 mM BisTris propane buffer, pH 7.5, at 25 °C. Observed rates were obtained by fitting to the single-exponential expression.

DISCUSSION

Structure−activity correlations have been routinely used to probe the nature of chemical intermediates in quinoprotein enzymes (*15*, *16*, *33*, *34*). We have recently shown that *para*-substituted benzylamines are inappropriate for probing the chemical mechanism of TTQ reduction in aromatic amine dehydrogenase (AADH) (*17*). With this in mind, we have isolated the TTQ-containing small subunit of AADH and investigated structure reactivity correlations with the subunit. The isolated small subunit exhibits a positive correlation of structure−reactivity data with electronic substituent effects, unlike structure−reactivity correlations for native enzyme and synthetic TTQ model compounds.

Reactions with synthetic TTQ (*20*), and other indolequinone derivatives (*21*, *22*), proceed with iminoquinone formation (k_1), followed by rearrangement to product-imine (k_2) and aminophenol formation (k_3) (*20*−*22*). Rate constants for reactions with conventional benzylamine are reported as 0.27 M^{-1} s^{-1} (k_1), 2.3 × 10^{-3} s^{-1} (k_2 with 20 mM substrate) and 2.7 × 10^{-2} M^{-1} s^{-1} (k_3) (*20*), which is considerably slower than the rate constant determined for reactions of the small subunit of AADH with benzylamine (1.9 ± 0.1 M^{-1} s^{-1}; Table 1). Structure activity relationships have been reported for reactions of synthetic TTQ with *para*-substituted benzylamines. Hammett plots of log k_1 and k_2 versus electronic effects (σ_p) exhibit a negative correlation (i.e., electron donating and electron withdrawing substituents enhance and decrease rate constants, respectively) (*20*). The opposite trend is observed with AADH (*17*), and herein with the TTQ-containing subunit of AADH, in which the most electron withdrawing group (nitro) activates bond cleavage and the most electron donating substituent (methyl group) yields the slowest rate for TTQ reduction (Table 4). The rearrangement step (iminoquinone to product imine) involves α-proton abstraction and electron flow from the α-carbon to the quinone moiety. The positive correlation for enzymatic reactions and σ_p has been attributed to enhancement of the α-proton abstraction step by electron withdrawing substituents (*15*, *20*), and the negative effect in the model system has been attributed to electron flow, from the α-carbon to the quinone moiety, being more difficult in the model system than in the enzymatic system (*20*). It is important to recognize in any discussion of the Hammett behavior of the synthetic TTQ center with that of the small subunit that these differences are most likely related to a change in mechanism. The amine in the synthetic model system is also playing the role of the active site base, and in this case, there is a substituent effect on both the substrate Schiff base and the proton abstracting base. This is unlikely the case for the small subunit in which the active site Asp residue is the probable base.

Although AADH and the small subunit behave similarly, with regard to the effect of substituents on the rate of TTQ reduction, we have observed a poor correlation of structure−reactivity data with electronic substituent effects for the native enzyme (i.e., Hammett plots deviate from linear

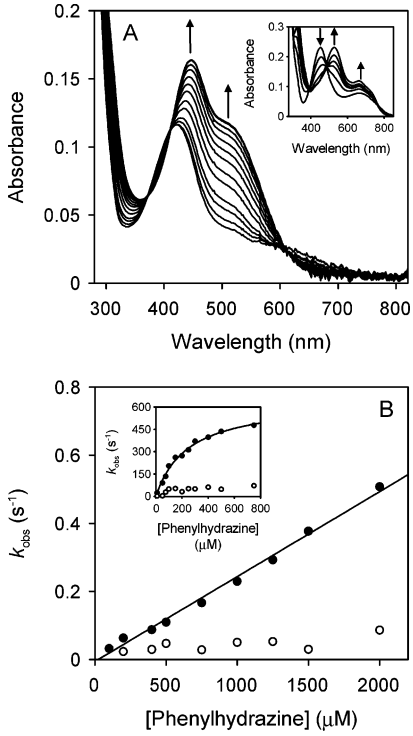

FIGURE 8: Kinetic studies of AADH and the small subunit with phenylhydrazine. Panel A: Spectral properties of the TTQ−phenylhydrazine complex in the small subunit of AADH. Spectral changes observed on addition of phenylhydrazine (20 μM) to the small subunit (10 μM) were followed spectrophotometrically. Inset: As main panel but for the addition of phenylhydrazine (16 μM) to AADH (8 μM). Panel B: Stopped-flow kinetic data for the formation of the TTQ−phenylhydrazine complex in the small subunit. Conditions: 4 μM small subunit, 10 mM BisTris propane buffer, pH 7.5, at 25 °C. Formation of the TTQ−phenylhydrazine complex was followed at 528 nm. Absorbance changes were biphasic, and observed rate constants were obtained by fitting to the standard double exponential expression. Filled circles, k_{obs1}; open circles, k_{obs2}. Inset: As main panel but for the formation of the TTQ−phenylhydrazine complex in AADH. Conditions: 2 μM AADH, 10 mM BisTris propane buffer, pH 7.5, 25 °C. The fit shown is to the standard hyperbolic expression.

behavior) (*17*). For reactions catalyzed by the small subunit, however, a stronger correlation of structure−reactivity data with electronic substituent effects is observed for *para*-substituted benzylamines and phenethylamines (Figure 6A−D). Our crystallographic studies of enzyme−substrate complexes of AADH and benzylamine substrates have identified that the formation of the benzylamine derived iminoquinone requires major structural reorganization in the active site, prior to C−H bond breakage, which compromises the rate of TTQ reduction (*17*). In contrast to the tryptamine (*9*) and phenylethanolamine (*14*)-derived iminoquinone complexes, the benzylamine-derived iminoquinone requires structural rearrangement of the benzyl side chain (stacked with Pheα169), which requires motions from the side chain of Pheα97 and the Aspα84 backbone (Figure 2) (*17*). The required reorganization is greater when larger substituents need to be accommodated in the active site, and thus a pronounced breakdown in structure−reactivity data with electronic substituent effects is observed for the native enzyme (*17*). Reactions of the subunit with *para*-substituted amines are not compromised by the large subunit, avoiding steric restrictions that occur in the active site of the native enzyme (Figure 9). As a result, no structural reorganization

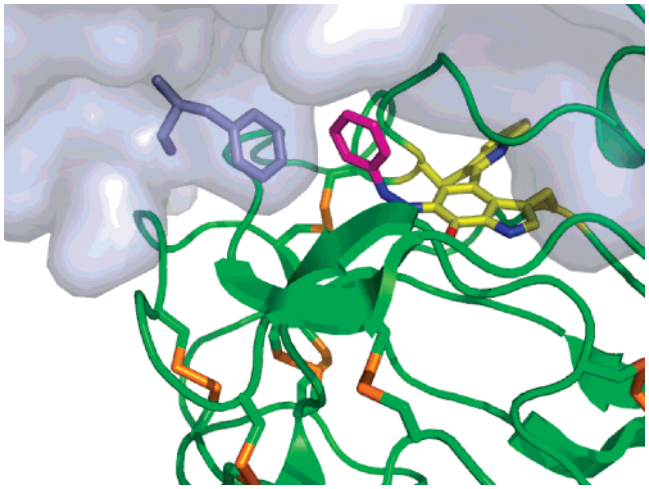

FIGURE 9: Representation of a single AADH heterodimer with molecular surface of the large subunit depicted as a blue transparent surface (made using PYMOL). The small subunit is shown in cartoon form with disulfide bonds, TTQ and phenylhydrazine inhibitor in atom colored sticks (cysteines with green, TTQ with yellow and substrate with magenta carbons). The position of Pheα97 is displayed as blue sticks. We propose that this residue in particular is responsible for the conformational gating (and hence deflated KIEs) observed with *para*-substituted benzylamines in the native enzyme.

is required and KIEs greater than unity are observed with the isolated small subunit (Figure 5A and Table 3). The absence of a well-defined substrate-binding site is consistent with TTQ reduction and hydrazone adduct formation in the small subunit being second order with respect to substrate (Figure 3C−F) and inhibitor (Figure 8) concentration, respectively. This is also consistent with the finding that TTQ reduction is observed for reactions of the small subunit with dimethoxybenzylamine but not for reactions with the native enzyme (Figure 7).

The isotope effect for C−H bond breakage in the TTQ model chemistry is large (~9), but studies of the temperature dependence of the KIE have not been reported (*20*). The extent of tunneling during H-transfer, and the involvement of gating motions in a tunneling reaction, are ascertained by measuring the temperature dependence of the KIE (*35*−*37*). If optimally evolved protein motions are not available, major differences in the temperature dependence of the KIE are expected (i.e., a switch from temperature independent, which indicates an optimally configured enzyme−substrate complex for H-tunneling, to a temperature-dependent KIE reflecting impaired tunneling or semiclassical transfer) (*35*−*38*). In reactions of AADH with tryptamine, substrate oxidation is dominated by H-tunneling and is accompanied by a highly inflated KIE (55) that is measurably independent of temperature ($\Delta\Delta H^{\ddagger}$ ~0 ± 5 kJ mol^{-1}) (*9*). Unlike thermodynamic parameters determined for the native enzyme (*8*, *9*, *17*), reactions of the small subunit are strongly dependent on temperature ($\Delta\Delta H^{\ddagger}$ ~10 ± 3 kJ mol^{-1}; Table 2). The exception is "faster" reactions with methylamine (50 mM) for which the KIE is, within error, measurably independent of temperature ($\Delta\Delta H^{\ddagger}$ 1.6 ± 3.4 kJ mol^{-1}; Table 2). The temperature-dependent KIEs could be indicative of impaired tunneling reactions, but given the deflated KIEs (~2.5 for tryptamine) we cannot exclude the possibility that the C−H bond breakage reaction may not be fully rate-limiting [as

for steady-state reactions of AADH with benzylamine, $\Delta\Delta H^{\ddagger} \sim 7 \pm 2$ kJ mol^{-1} (*26*)].[5]

The question of which factors promote enzyme catalysis is one of the most difficult to address experimentally. Several studies have demonstrated a role for protein motion in facilitating tunneling (*11*, *35*, *39*, *40*), but others have argued that motions which contribute to tunneling are similar in both enzymes and free solution (*41*−*43*). Atomic level detail of the reaction catalyzed by the TTQ-containing subunit of AADH is required to provide insight into the mechanistic origin of the observed isotope effects, and identify a role (if any) for quantum mechanical H-transfer. Our work with the native enzyme (*17*) has emphasized the importance of structural analyses to probe for alternate (suboptimal) geometries that might impact on reactivity. In this study, we have demonstrated that the kinetic properties of the reaction catalyzed by the TTQ-containing subunit of AADH are distinct from the native enzyme, and that *para*-substituted benzylamines are good reactivity probes of TTQ mechanism with the isolated small subunit. Further analysis of this system, through combined computational and structural studies, will allow us to rigorously probe a potential role for short- and long-range coupled motions in facilitating the enzyme chemistry as well as understand what dynamic changes lead to impaired catalytic properties.

ACKNOWLEDGMENT

We thank Dr. Khalid Abu Khadra for investigating methods for the isolation of the catalytic subunit.

SUPPORTING INFORMATION AVAILABLE

NOESY spectrum from NMR studies of the isolated small subunit (Figure S1). Steady-state kinetic data for reactions of the small subunit with methylamine as substrate (Figure S2). Eyring plots for reactions of the small subunit with amine substrates (Figure S3). This material is available free of charge via the Internet at http://pubs.acs.org.

REFERENCES

1. Govindaraj, S., Eisenstein, E., Jones, L. H., Sanders-Loehr, J., Chistoserdov, A. Y., Davidson, V. L., and Edwards, S. L. (1994) Aromatic amine dehydrogenase, a second tryptophan tryptophylquinone enzyme, *J. Bacteriol. 176*, 2922−2929.
2. Davidson, V. L. (2005) Structure and mechanism of tryptophylquinone enzymes, *Bioorg. Chem. 33*, 159−170.
3. Davidson, V. L. (1993) *Principles and Applications of Quinoproteins* (Davidson, V. L., Ed.), pp 73−95, Marcel Dekker, Inc., New York.
4. Husain, M., and Davidson, V. L. (1987) Purification and properties of methylamine dehydrogenase from *Paracoccus denitrificans*, *J. Bacteriol. 169*, 1712−1717.
5. McIntire, W. S., Wemmer, D. E., Chistoserdov, A., and Lidstrom, M. E. (1991) A new cofactor in a prokaryotic enzyme: tryptophan tryptophylquinone as the redox prosthetic group in methylamine dehydrogenase, *Science 252*, 817−824.
6. Chistoserdov, A. Y., Tsygankov, Y. D., and Lidstrom, M. E. (1990) Cloning and sequencing of the structural gene for the small subunit of methylamine dehydrogenase from *Methylobacterium extorquens* AM1: evidence for two tryptophan residues involved in the active center, *Biochem. Biophys. Res. Commun. 172*, 211−216.
7. Basran, J., Sutcliffe, M. J., and Scrutton, N. S. (1999) Enzymatic H-transfer requires vibration-driven extreme tunneling, *Biochemistry 38*, 3218−3222.
8. Basran, J., Patel, S., Sutcliffe, M. J., and Scrutton, N. S. (2001) Importance of barrier shape in enzyme-catalyzed reactions. Vibrationally assisted hydrogen tunneling in tryptophan tryptophylquinone-dependent amine dehydrogenases, *J. Biol. Chem. 276*, 6234−6242.
9. Masgrau, L., Roujeinikova, A., Johannissen, L. O., Hothi, P., Basran, J., Ranaghan, K. E., Mulholland, A. J., Sutcliffe, M. J., Scrutton, N. S., and Leys, D. (2006) Atomic description of an enzyme reaction dominated by proton tunneling, *Science 312*, 237−241.
10. Masgrau, L., Ranaghan, K. E., Scrutton, N. S., Mulholland, A. J., and Sutcliffe, M. J. (2007) Tunneling and classical paths for proton transfer in an enzyme reaction dominated by tunneling: oxidation of tryptamine by aromatic amine dehydrogenase, *J. Phys. Chem. B 111*, 3032−3047.
11. Johannissen, L. O., Hay, S., Scrutton, N. S., and Sutcliffe, M. J. (2007) Proton tunneling in aromatic amine dehydrogenase is driven by a short-range sub-picosecond promoting vibration: consistency of simulation and theory with experiment, *J. Phys. Chem. B 111*, 2631−2638.
12. Hyun, Y. L., and Davidson, V. L. (1995) Electron transfer reactions between aromatic amine dehydrogenase and azurin, *Biochemistry 34*, 12249−12254.
13. Roujeinikova, A., Scrutton, N. S., and Leys, D. (2006) Atomic level insight into the oxidative half-reaction of aromatic amine dehydrogenase, *J. Biol. Chem. 281*, 40264−40272.
14. Roujeinikova, A., Hothi, P., Masgrau, L., Sutcliffe, M. J., Scrutton, N. S., and Leys, D. (2007) New insights into the reductive half-reaction mechanism of aromatic amine dehydrogenase revealed by reaction with carbinolamine substrates, *J. Biol. Chem. 282*, 23766−23777.
15. Hyun, Y. L., and Davidson, V. L. (1995) Mechanistic studies of aromatic amine dehydrogenase, a tryptophan tryptophylquinone enzyme, *Biochemistry 34*, 816−823.
16. Davidson, V. L., Jones, L. H., and Graichen, M. E. (1992) Reactions of benzylamines with methylamine dehydrogenase. Evidence for a carbanionic reaction intermediate and reaction mechanism similar to eukaryotic quinoproteins, *Biochemistry 31*, 3385−3390.
17. Hothi, P., Roujeinikova, A., Khadra, K. A., Lee, M., Cullis, P., Leys, D., and Scrutton, N. S. (2007) Isotope effects reveal that *para*-substituted benzylamines are poor reactivity probes of quinoprotein mechanism for aromatic amine dehydrogenase, *Biochemistry 46*, 9250−9259.
18. Itoh, S., Ogino, M., Komatsu, M., and Ohshiro, Y. (1992) Synthesis and characterization of the model compound of active site cofactor TTQ of bacterial methylamine dehydrogenases, *J. Am. Chem. Soc. 114*, 7294−7295.
19. Itoh, S., Ogino, M., Haranou, S., Terasaka, T., Ando, T., Komatsu, M., Ohshiro, Y., Fukuzumi, S., Kano, K., Takagi, K., and Ikeda, T. (1995) A model compound of the novel cofactor tryptophan tryptophylquinone of bacterial methylamine dehydrogenases. Synthesis and physicochemical properties, *J. Am. Chem. Soc. 117*, 1485−1493.
20. Itoh, S., Takada, N., Haranou, S., Ando, T., Komatsu, M., Ohshiro, Y., and Fukuzumi, S. (1996) Model studies of TTQ-containing amine dehydrogenases, *J. Org. Chem. 61*, 8967−8974.
21. Itoh, S., Takada, N., Ando, T., Haranou, S., Huang, X., Uenoyama, Y., Ohshiro, Y., Komatsu, M., and Fukuzumi, S. (1997) Synthesis, physicochemical properties, and amine-oxidation reaction of indolequinone derivatives as model compounds of novel organic cofactor TTQ of amine dehydrogenases, *J. Org. Chem. 62*, 5898−5907.
22. Itoh, S., Taniguchi, M., Takada, N., Nagatomo, S., Kitagawa, T., and Fukuzumi, S. (2000) Effects of metal Ions on the electronic, redox, and catalytic properties of cofactor TTQ of quinoprotein amine dehydrogenases, *J. Am. Chem. Soc. 122*, 12087−12097.
23. Murakami, Y., Yoshimoto, N., Fujieda, N., Ohkubo, K., Hasegawa, T., Kano, K., Fukuzumi, S., and Itoh, S. (2007) Model studies of 6,7-indolequinone cofactors of quinoprotein amine dehydrogenases, *J. Org. Chem. 72*, 3369−3380.
24. Brooks, H. B., Jones, L. H., and Davidson, V. L. (1993) Deuterium kinetic isotope effect and stopped-flow kinetic studies of the quinoprotein methylamine dehydrogenase, *Biochemistry 32*, 2725−2729.

[5] Additionally, although KIEs with benzylamines are elevated with the small subunit compared with native AADH, we cannot be entirely certain that C−H bond breakage is fully rate limiting.

25. Iwaki, M., Yagi, T., Horiike, K., Saeki, Y., Ushijima, T., and Nozaki, M. (1983) Crystallization and properties of aromatic amine dehydrogenase from *Pseudomonas* sp, *Arch. Biochem. Biophys. 220*, 253−262.
26. Hothi, P., Khadra, K. A., Combe, J. P., Leys, D., and Scrutton, N. S. (2005) Tryptophan tryptophylquinone cofactor biogenesis in the aromatic amine dehydrogenase of *Alcaligenes faecalis*. Cofactor assembly and catalytic properties of recombinant enzyme expressed in *Paracoccus denitrificans*, *FEBS J. 272*, 5894−5909.
27. Kenney, W. C., and McIntire, W. S. (1983) Characterization of methylamine dehydrogenase from Bacterium W3A1. Interaction with reductants and amino-containing compounds, *Biochemistry 22*, 3858−3868.
28. Strickland, S., Palmer, G., and Massey, V. (1975) Determination of dissociation constants and specific rate constants of enzyme-substrate (or protein-ligand) interactions from rapid reaction kinetic data, *J. Biol. Chem. 250*, 4048−4052.
29. Hansch, C., Leo, A. (1979) *Correlation Analysis in Chemistry and Biology*, Wiley-Interscience, New York.
30. Hansch, C., Leo, A., and Taft, R. W. (1991) A survey of Hammett substituent constants and resonance and field parameters, *Chem. Rev. 91*, 165−195.
31. Silverman, R. B. (1988) *Chemistry and Enzymology*, pp 158−167, CRC Press, Boca Raton.
32. Davidson, V. L., and Jones, L. H. (1992) Cofactor-directed inactivation by nucleophilic amines of the quinoprotein methylamine dehydrogenase from *Paracoccus denitrificans*, *Biochim. Biophys. Acta 1121*, 104−110.
33. Williamson, P. R., and Kagan, H. M. (1987) Electronegativity of aromatic amines as a basis for the development of ground state inhibitors of lysyl oxidase, *J. Biol. Chem. 262*, 14520−14524.
34. Hartmann, C., and Klinman, J. P. (1991) Structure-function studies of substrate oxidation by bovine serum amine oxidase: relationship to cofactor structure and mechanism, *Biochemistry 30*, 4605−4611.
35. Knapp, M. J., and Klinman, J. P. (2002) Environmentally coupled hydrogen tunneling. Linking catalysis to dynamics, *Eur. J. Biochem. 269*, 3113−3121.
36. Kohen, A. (2003) Kinetic isotope effects as probes for hydrogen tunneling, coupled motion and dynamics contributions to enzyme catalysis, *Prog. React. Kinet. Mech. 28*, 119−156.
37. Masgrau, L., Basran, J., Hothi, P., Sutcliffe, M. J., and Scrutton, N. S. (2004) Hydrogen tunneling in quinoproteins, *Arch. Biochem. Biophys. 428*, 41−51.
38. Sutcliffe, M. J., and Scrutton, N. S. (2006) Computational studies of enzyme mechanism: linking theory with experiment in the analysis of enzymic H-tunnelling, *Phys. Chem. Chem. Phys. 8*, 4510−4516.
39. Agarwal, P. K., Billeter, S. R., Rajagopalan, P. T., Benkovic, S. J., and Hammes-Schiffer, S. (2002) Network of coupled promoting motions in enzyme catalysis, *Proc. Natl. Acad. Sci. U.S.A. 99*, 2794−2799.
40. Caratzoulas, S., Mincer, J. S., and Schwartz, S. D. (2002) Identification of a protein-promoting vibration in the reaction catalyzed by horse liver alcohol dehydrogenase, *J. Am. Chem. Soc. 124*, 3270−3276.
41. Olsson, M. H. M., Siegbahn, P. E. M., and Warshel, A. (2004) Simulations of the large kinetic isotope effect and the temperature dependence of the hydrogen atom transfer in lipoxygenase, *J. Am. Chem. Soc. 126*, 2820−2828.
42. Siebrand, W., and Smedarchina, Z. (2004) Temperature dependence of kinetic isotope effects for enzymatic carbon-hydrogen bond cleavage, *J. Phys. Chem. B 108*, 4185−4195.
43. Doll, K. M., Bender, B. R., and Finke, R. G. (2003) The first experimental test of the hypothesis that enzymes have evolved to enhance hydrogen tunneling, *J. Am. Chem. Soc. 125*, 10877−10884.

BI701690U